AIAA JOURNAL
Vol. 34, No. 7, July 1996

Near-Limit Oscillations of Spherical Diffusion Flames

S. Cheatham* and M. Matalon†
Northwestern University, Evanston, Illinois 60208-3125

We examine the dynamic characteristics of the diffusion flame surrounding a droplet of liquid fuel in a reduced oxidant environment. The study is motivated by the experimental observations of candle flames in microgravity, which bear some similarity to the spherical diffusion flame that surrounds a burning liquid fuel droplet. The microgravity experiments reveal that, when the oxidant concentration in the chamber is sufficiently low, oscillations develop before extinction. A similar phenomenon is predicted here. An oscillatory state results for a sufficiently low oxidant concentration when radiative losses from the flame are appreciable. The frequencies of oscillations we predict are in good agreement with the experimental observations.

Nomenclature

A = frequency factor of the chemical reaction rate
a = droplet radius
c_p = specific heat at constant pressure
D = Damköhler number, $(A\rho_\infty a^2/\mathcal{D}_{th})(Y_\ell/\nu_F W_F)$
$\mathcal{D}_i$ = molecular diffusivity of species i
$\mathcal{D}_{th}$ = thermal diffusivity of the mixture, $\lambda/\rho_\infty c_p$
E = activation energy
h = heat loss parameter, $16T_\infty^3 a^2\sigma/\lambda\ell_p\epsilon^2$
L = latent heat of vaporization (dimensionless)
L_i = Lewis number of species i, $\mathcal{D}_{th}/\mathcal{D}_i$
ℓ_p = Planck mean absorption length
M = mass flow rate, $r^2\rho v$
Q = total chemical heat released (per unit mass of the mixture)
q = dimensionless heat release parameter, $(Q/c_pT_\infty)(Y_\ell/\nu_F W_F)$
R = scaled radial distance
R^0 = gas constant
r = radial coordinate
T = temperature
T_s = dimensionless surface temperature
t = time
v = radial velocity
W_i = molecular weight of species i
X = oxidant mass fraction
Y = fuel mass fraction
γ = scaled oxidant concentration of ambient, $\epsilon^{-1}X_\infty/\nu Y_\ell$
δ = reduced Damköhler number, $D\epsilon^{-1}e^{-1/\epsilon}$
ϵ = reciprocal activation energy parameter, R^0T_∞/E
λ = thermal conductivity of the mixture
ν = ratio of mass weighted stoichiometric coefficients, $\nu_X W_X/\nu_F W_F$
ν_i = stoichiometric coefficient for species i
ρ = density of the mixture
σ = Stefan–Boltzmann coefficient

Subscripts

F = fuel
ℓ = liquid
s = steady state
X = oxidant
∞ = ambient

Received Oct. 27, 1995; presented as Paper 96-0260 at the AIAA 34th Aerospace Sciences Meeting, Reno, NV, Jan. 10–12, 1996; revision received March 6, 1996; accepted for publication March 13, 1996.

*Graduate Student, Department of Engineering Sciences and Applied Mathematics, 2145 Sheridan Road.
†Professor, McCormick School of Engineering and Applied Science, 2145 Sheridan Road. Senior Member AIAA.

I. Introduction

FROM recent experiments of candle flames conducted in a reduced gravity environment,[1,2] the following observations were made: The flame shape is nearly a hemisphere, as opposed to the elongated teardrop shape observed under normal gravity conditions. The flame standoff distance is quite large; at the base of the flame that distance is about 5–8 mm, compared with 1–2 mm in normal gravity conditions. The burning rate and the flame temperature are considerably reduced when compared with their values in normal gravity. The flame is quasisteady during most of the process, but as the oxygen in the chamber is nearly consumed, spontaneous oscillations develop before extinction. The goal of this work is to shed light on these observations and in particular on the oscillations that occur during the last stages of the burning.

The candle flame in microgravity bears some similarity to the diffusion flame that surrounds a burning liquid droplet. Both have a spherical shape and both depend on the heat conducted back to the condensed phase. Hence their structure and dynamical properties are likely to be similar. In our attempt to model the preceding observations, we have therefore analyzed the droplet problem. To simulate the experimental conditions we consider the burning to occur in a reduced oxidant environment; i.e., the ambient mass fraction of the oxidant X_∞ is assumed small. Under these conditions the flame standoff distance is relatively large and the burning rate is relatively low. The combustion field is now divided into a near field, where fuel vapor in the absence of oxidant is transported outward by convection and diffusion, and a broad chemically reactive far field, where convection is effectively negligible, but radiative heat loss is important.

The dependence of the burning rate on the Damköhler number, representing the ratio of the diffusion time to the chemical reaction time, has different characteristics depending on whether the oxidant concentration in the ambient environment is low or not. In a reduced oxidant environment, the transition from intense burning to a nearly frozen state occurs in a gradual way in contrast to the abrupt change that typifies the familiar S-shaped response curve. The transitional states, however, are not always stable. In the absence of radiative losses from the flame and for unity Lewis numbers, the transitional states are stable to spherically symmetric small disturbances. For unity Lewis numbers, instabilities associated with oscillatory combustion may occur when radiative losses become sufficiently large. The effect of nonunity Lewis numbers will be examined in a following paper. For typical values of the parameters the frequency of the predicted oscillations is in the range of 0.7–1.5 Hz, which compares well with the measured frequencies observed in the candle flame experiment. Given the similarity between the droplet combustion problem and the candle flame, it is reasonable to expect that the intrinsic instability discovered here plays some role in the observed near-limit oscillations. The candle flame experiment is clearly more complicated, and such factors as pressure oscillations in the combustion chamber or capillary effects along the wick, which are excluded in the theory, may have significant influence on the overall flame dynamics.

The steady problem in the absence of heat loss and with a unity Lewis number has been previously discussed in Ref. 3. Stability discussions, however, are limited: in Ref. 4 it was shown that for nonunity Lewis numbers and/or in the presence of heat loss oscillations develop near the extinction limit for an S-shaped response, whereas in a recent study[5] consideration was given to the edge flame, and it was shown that oscillations could occur when the effective Lewis number is sufficiently large.

II. Formulation

A spherical liquid fuel droplet is burning quasisteadily in a reduced oxidant environment. The temperature of the liquid is assumed to remain constant and is approximately equal to the boiling temperature T_ℓ. The fuel mass fraction of the droplet is Y_ℓ. Far from the droplet the temperature $T_\infty > T_\ell$ so that heat conducted back to the droplet vaporizes the liquid fuel and provides the fuel vapor that burns with the ambient oxidant. We are specifically concerned in this study with situations in which the mass fraction of the oxidant in the ambient, X_∞, is small. The chemical reaction in the gas phase is modeled by a simple one-step irreversible reaction of the form

$$\nu_F F + \nu_X O \rightarrow \text{Products}$$

The temperature dependence of the reaction rate is taken to be of Arrhenius type with a frequency factor A and an overall activation energy E. The radiant energy loss from the flame is expressed in the form $4\sigma(T^4 - T_\infty^4)/\ell_p$. This expression is based on a simple phenomenological model valid for an optically thin gas.[6] Since radiation from the flame is principally from excited molecular fragments of intermediate species and from combustion products, the length ℓ_p should be such that the factor $1/\ell_p \rightarrow 0$ when the reaction rate is weak.

Appropriate equations[7] governing the burning process are

$$\epsilon^2 \frac{\partial \rho}{\partial t} + \frac{1}{r^2}\frac{\partial}{\partial r}(r^2 \rho v) = 0 \tag{1}$$

$$\epsilon^2 \rho \frac{\partial T}{\partial t} + \rho v \frac{\partial T}{\partial r} - \frac{1}{r^2}\frac{\partial}{\partial r}\left(r^2 \frac{\partial T}{\partial r}\right) = q\rho^2 DXY e^{-1/\epsilon T} - \epsilon^2 \frac{h}{4}(T^4 - 1) \tag{2}$$

$$\epsilon^2 \rho \frac{\partial Y}{\partial t} + \rho v \frac{\partial Y}{\partial r} - L_F^{-1}\frac{1}{r^2}\frac{\partial}{\partial r}\left(r^2 \frac{\partial Y}{\partial r}\right) = -\rho^2 DXY e^{-1/\epsilon T} \tag{3}$$

$$\epsilon^2 \rho \frac{\partial X}{\partial t} + \rho v \frac{\partial X}{\partial r} - L_X^{-1}\frac{1}{r^2}\frac{\partial}{\partial r}\left(r^2 \frac{\partial X}{\partial r}\right) = -\rho^2 DXY e^{-1/\epsilon T} \tag{4}$$

$$\rho T = 1 \tag{5}$$

These equations are made dimensionless using the ambient conditions ρ_∞ and T_∞ as units for the density and temperature, the droplet radius a as a unit of length, $\mathcal{D}_{th}/a$ as a unit of velocity with $\mathcal{D}_{th} = \lambda/\rho_\infty c_p$, and $(a^2/\mathcal{D}_{th})(E/R^0 T_\infty)^2$ as a unit of time (this particular choice in scaling time will be clarified later). The fuel and oxidant mass fractions Y and X have been normalized with Y_ℓ and νY_ℓ, respectively. The parameters in these equations are, therefore, the reciprocal activation energy ϵ, the heat release parameter q, the heat loss parameter h, the Lewis numbers L_F and L_X and the Damköhler number D.

The boundary conditions at the droplet surface, $r = 1$, are

$$\begin{aligned} \rho v Y - L_F^{-1}\frac{\partial Y}{\partial r} &= \rho v, & \rho v X - L_X^{-1}\frac{\partial X}{\partial r} &= 0 \\ \frac{\partial T}{\partial r} &= \rho v L, & T &= T_s \end{aligned} \tag{6}$$

where L is measured in units of $c_p T_\infty$.

Far from the droplet, i.e., as $r \rightarrow \infty$, we expect that

$$v \rightarrow 0, \qquad T \rightarrow 1, \qquad Y \rightarrow 0, \qquad X \rightarrow \epsilon\gamma \tag{7}$$

where $\gamma = \epsilon^{-1} X_\infty / \nu Y_\ell$. Regarding the fuel's concentration we shall impose the stricter requirement that the total flux vanishes, i.e.,

$$\lim_{r\rightarrow\infty}\left(4\pi r^2 \frac{\partial Y}{\partial r}\right) = 0 \tag{8}$$

implying that all of the fuel has been consumed as a result of combustion.

III. Asymptotic Treatment

In the following we consider the limit of large activation energy, or $\epsilon \ll 1$. The reaction term in this case is exponentially small except in regions where $T \simeq 1$; then it could be appreciable if the Damköhler number $D \sim \epsilon \exp(1/\epsilon)$. The combustion field is therefore effectively divided into two regions. A frozen near field, adjacent to the droplet, where fuel vapor is transported outward by convection and diffusion, and a relatively broad chemically reactive far field at an $\mathcal{O}(\epsilon^{-1})$ distance from the droplet where convection is negligible. The scaling of the time variable ensures that the near field remains quasisteady; transient effects become important only in the reactive far field. Similar scaling has been encountered before[8,9] in related problems. Radiative loss is also important in the far field where chemical reaction occurs, and as remarked earlier, the heat loss parameter h must go to zero when the Damköhler number D is small. Finally, we note that the scaling considered here reflects the fact that X_∞ is small, so that γ remains an $\mathcal{O}(1)$ quantity.

A. Near Field

For $r \sim \mathcal{O}(1)$ distances, we expand all variables in the form $T = T_0 + \epsilon T_1 + \cdots$. The resulting linear equations are then solved subject to the boundary conditions (6). To leading order, the solution is expected to have the behavior (7) as $r \rightarrow \infty$. Thus, correct to $O(\epsilon)$, one finds the solution

$$T \sim T_s - L + (1 - T_s + L)\, e^{-M_0/r} + \epsilon M_1 (1 - T_s + L)[1 - (1/r)]e^{-M_0/r} + \cdots \tag{9}$$

$$Y \sim 1 - e^{-L_F M_0/r} + \epsilon\{L_F(M_1/r) + C_F\}e^{-L_F M_0/r} + \cdots \tag{10}$$

$$X \sim \epsilon C_X e^{-L_X M_0/r} + \cdots \tag{11}$$

where the mass flow rate $M \equiv r^2 \rho v$ has also been expanded as $M = M_0 + \epsilon M_1 + \cdots$. Since the temperature in the far field remains near $T = 1$, the mass flow rate, to leading order, corresponds to that of pure vaporization, namely,

$$M_0 = \ell_n\{1 + [(1 - T_s)/L)]\}$$

The correction term that accounts for burning, M_1, remains to be determined, and so do the constants of integration C_F and C_X.

B. Far Field

The description of the far field requires rescaling the radial distance by writing $r = R/\epsilon$. Introducing the expansions

$$T = 1 + \epsilon\phi(R, t) + \cdots \qquad Y = \epsilon y(R, t) + \cdots$$

$$X = \epsilon x(R, t) + \cdots \qquad M = m(R, t) + \cdots$$

the governing equations (1–4) simplify to

$$-\frac{\partial \phi}{\partial t} + \frac{1}{R^2}\frac{\partial m}{\partial R} = 0 \tag{12}$$

$$\frac{\partial \phi}{\partial t} - \frac{1}{R^2}\frac{\partial}{\partial R}\left(R^2 \frac{\partial \phi}{\partial R}\right) = q\delta xy e^{\phi} - h\phi \tag{13}$$

$$\frac{\partial y}{\partial t} - L_F^{-1}\frac{1}{R^2}\frac{\partial}{\partial R}\left(R^2 \frac{\partial y}{\partial R}\right) = -\delta xy e^{\phi} \tag{14}$$

$$\frac{\partial x}{\partial t} - L_X^{-1}\frac{1}{R^2}\frac{\partial}{\partial R}\left(R^2 \frac{\partial x}{\partial R}\right) = -\delta xy e^{\phi} \tag{15}$$

where $\delta = D\epsilon^{-1}e^{-1/\epsilon} = \mathcal{O}(1)$ is the reduced Damköhler number. We observe that, in the far field, diffusion, chemical reaction, and radiative loss are the dominant processes, whereas convection is negligibly small.

Since Eq. (12) is uncoupled from the rest, it serves to determine m a posteriori. Hence, in the following, we concentrate on Eqs. (13–15).

Matching with the near field solution (9–11) requires that

$$\begin{aligned} \phi &\sim (1 + L - T_s)[-(M_0/R) + M_1] + o(1) \\ y &\sim L_F\frac{M_0}{R} + C_F + o(1), \qquad x \sim C_X + o(1) \end{aligned} \tag{16}$$

as $R \to 0$. The other boundary conditions are

$$\phi \to 0, \qquad x \to \gamma, \qquad R^2\frac{\partial y}{\partial R} \to 0 \tag{17}$$

as $R \to \infty$; the last results from Eq. (8). These conditions are sufficient for the determination of the solution including the quantities M_1, C_F, and C_X.

Finally we note that, viewed on this length scale, the droplet is effectively a sink of energy and a source of fuel vapor. The conditions (16) determine the appropriate fluxes to and from the droplet, corresponding to pure vaporization of the liquid fuel.

IV. Steady States

In the absence of the time-dependent terms, Eqs. (14) and (15) can be subtracted so as to eliminate the nonlinear term. The resulting equation can be integrated to give

$$L_X^{-1}x_s - L_F^{-1}y_s = -(M_0/R) + L_X^{-1}\gamma \tag{18}$$

together with the relation $C_X = \gamma + L_X L_F^{-1} C_F$. The remaining equations simplify to

$$\frac{1}{R^2}\frac{\mathrm{d}}{\mathrm{d}R}\left(R^2\frac{\mathrm{d}\phi_s}{\mathrm{d}R}\right) = -q\delta\, L_X\, y_s\left(L_F^{-1}y_s - \frac{M_0}{R} + L_X^{-1}\gamma\right)e^{\phi_s} + h\phi_s \tag{19}$$

$$L_F^{-1}\frac{1}{R^2}\frac{\mathrm{d}}{\mathrm{d}R}\left(R^2\frac{\mathrm{d}y_s}{\mathrm{d}R}\right) = \delta\, L_X\, y_s\left(L_F^{-1}y_s - \frac{M_0}{R} + L_X^{-1}\gamma\right)e^{\phi_s} \tag{20}$$

For the solution of these equations it suffices to impose the conditions

$$\begin{aligned} &\frac{\mathrm{d}\phi_s}{\mathrm{d}R} = (1 - T_s + L)\frac{M_0}{R^2}, \qquad \frac{\mathrm{d}y_s}{\mathrm{d}R} = -L_F\frac{M_0}{R^2} \quad \text{as} \quad R \to 0 \\ &\phi_s \to 0, \qquad R^2\frac{\partial y_s}{\partial R} \to 0 \quad \text{as} \quad R \to \infty \end{aligned} \tag{21}$$

The complete matching conditions (16) are then used to determine the constants M_1, C_F, and C_O. In particular we are interested in the response of the correction to the burning rate M_1 to variations in the reduced Damköhler number δ and the oxidant concentration γ.

It is convenient for numerical integration to use the asymptotic behavior of ϕ_s and y_s for large R, which can be deduced from the solution of the limiting equations. These take the form

$$\begin{aligned} &\frac{\mathrm{d}\phi_s}{\mathrm{d}R} + \left(\frac{1}{R} + \sqrt{h}\right)\phi_s \sim \left(\frac{\delta\gamma q}{\sqrt{\delta\gamma L_F} + \sqrt{h}}\right)y_s \\ &\frac{\mathrm{d}y_s}{\mathrm{d}R} + \left(\frac{1}{R} + \sqrt{\delta\gamma L_F}\right)y_s \sim 0 \end{aligned}$$

as $R \to \infty$.

It is instructive to examine first the limits of small and large values of δ for which analytical expressions can be written for the solution. The numerical results complement these results for intermediate values of δ.

A. Small δ

The requirement that radiation from the reaction zone must vanish when $\delta \to 0$ necessitates writing $h = \delta\hat{h}$ with $\hat{h} = \mathcal{O}(1)$. Because the chemical activity is weak, the reactive-diffusive zone is now further away from the droplet, which requires rescaling the distance R. Writing $R = \delta^{-1/2}\xi$, and consequently $y_s \sim \delta^{1/2}y_s^*$ and $\phi_s = \delta^{1/2}\phi_s^*$, the governing equations reduce to

$$\begin{aligned} &L_F^{-1}\frac{1}{\xi^2}\frac{\mathrm{d}}{\mathrm{d}\xi}\left(\xi^2\frac{\mathrm{d}y_s^*}{\mathrm{d}\xi}\right) = \gamma y_s^* \\ &\frac{1}{\xi^2}\frac{\mathrm{d}}{\mathrm{d}\xi}\left(\xi^2\frac{\mathrm{d}\phi_s^*}{\mathrm{d}\xi}\right) = -\gamma q y_s^* + \hat{h}\phi_s^* \end{aligned}$$

The chemical reaction occurs here under effectively isothermal conditions ($\phi_s \sim 0$), and the oxidant consumption is negligibly small ($x_s \sim \gamma$). The solution

$$y_s^* = L_F M_0\frac{e^{-\sqrt{\gamma L_F}\xi}}{\xi}$$

$$\phi_s^* = -M_0(1 - T_s + L)\frac{e^{-\sqrt{\hat{h}}\xi}}{\xi} + \frac{\gamma q M_0 L_F}{\gamma L_F - \hat{h}}\left[\frac{e^{-\sqrt{\hat{h}}\xi}}{\xi} - \frac{e^{-\sqrt{\gamma L_F}\xi}}{\xi}\right]$$

implies that the burning rate correction is

$$M_1 = \delta^{1/2}\left[(\sqrt{\gamma L_F} + \sqrt{\hat{h}})^{-1}\frac{\gamma q L_F M_0}{1 - T_s + L} + \sqrt{\hat{h}}M_0\right] \tag{22}$$

B. Large δ

The limit $\delta \to \infty$ results in a Burke–Schumann flame sheet separating a region where there is fuel but no oxidant, from a region where there is only oxidant. If the flame sheet is located at $R = R_f$, then $x_s \equiv 0$ for $R < R_f$ and $y_s \equiv 0$ for $R > R_f$. The solution of Eqs. (19) and (20) that satisfies continuity at the flame sheet and the requirement that fuel and oxidant flow into the reaction zone in stoichiometric proportions is

$$\phi_s = \begin{cases} -M_0(1 - T_s + L)\dfrac{e^{-\sqrt{h}R}}{R} + \dfrac{qM_0e^{-\sqrt{h}R_f}}{\sqrt{h}R_f}\dfrac{\sinh\sqrt{h}R}{R} & \\ \qquad\qquad\qquad\qquad\qquad\qquad\qquad\qquad R < R_f & \\ \left[-M_0(1 - T_s + L) + \dfrac{qM_0}{\sqrt{h}R_f}\sinh\sqrt{h}R_f\right]\dfrac{e^{-\sqrt{h}R}}{R} & \\ \qquad\qquad\qquad\qquad\qquad\qquad\qquad\qquad R > R_f & \end{cases}$$

$$y_s = \begin{cases} L_F[(M_0/R) - L_X^{-1}\gamma] & R < R_f \\ 0 & R > R_f \end{cases}$$

$$x_s = \begin{cases} 0 & R < R_f \\ -L_X(M_0/R) + \gamma & R > R_f \end{cases}$$

where $R_f = M_0L_X/\gamma$. It can be verified that there is a reduction in the flame temperature $\phi_s(R_f)$ as a result of the heat loss from the reaction zone. Finally, matching as $R \to 0$ yields

$$M_1 \sim \frac{\gamma q L_X^{-1}}{1 - T_s + L}\exp(-\sqrt{h}L_X M_0/\gamma) + \sqrt{h}M_0 \tag{23}$$

C. Response Curves

Both expressions, Eq. (22) for small δ and Eq. (23) for large δ, show that the effect of radiation is twofold. On one hand there is a reduction in M_1, when compared with the case $h = 0$, that results from the heat loss from the reaction zone by radiation. On the other hand, there is an increase in M_1 associated with the enhancement in the vaporization rate caused by the radiative heat transferred to the near field. We note that because of these competing effects it is possible for M_1 to exceed the asymptotic value (23) at some intermediate δ. For moderate values of δ, the system (19–21) was solved numerically using the boundary value solver COLSYS. Representative profiles of ϕ_s, y_s, and x_s are shown in Fig. 1 for two different values of δ/q. A broad reaction zone with a reduced flame temperature is found for the lower value of δ. In contrast, the solution for the larger value of δ approaches the Burke–Schumann flame sheet solution with complete consumption of both reactants. Response curves showing the dependence of the correction to the burning rate M_1 on δ/q are shown in Fig. 2 for several values of the oxidant concentration γ. (Here M_1 has been scaled so that its normalized value μ tends to 1 as $\delta \to \infty$.) Note that, as predicted by Eq. (22), $M_1 \sim \delta^{1/2}$ for small δ. The figure reveals that the response curve takes on different shapes depending on the value of γ or the oxidant concentration in the ambient. For sufficiently large values of γ, the familiar S-shaped response curve is recovered. However, for

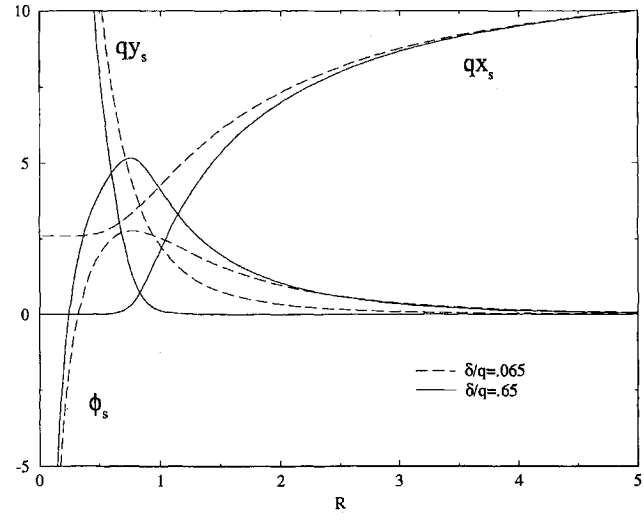

Fig. 1 Profiles of temperature and mass fraction perturbations for two values of δ/q. Calculated for $M_0(1 - T_s + L) = 2, qM_0 = 10, \gamma q = 12$, and $h = 0.5$.

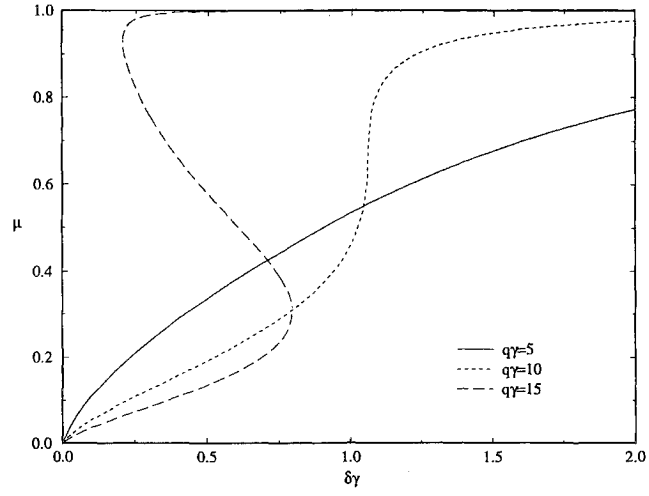

Fig. 2 Response curves: correction to the burning rate as a function of the Damköhler number δ, for selected values of γq. Calculated for $h = 0.05$ and several values of $\gamma \sim X_\infty$. Here $\mu = (L_X/\gamma q)(M_1 - \sqrt{hM_0})(1 - T_s + L)e^{\sqrt{hL_XM_0}/\gamma}$.

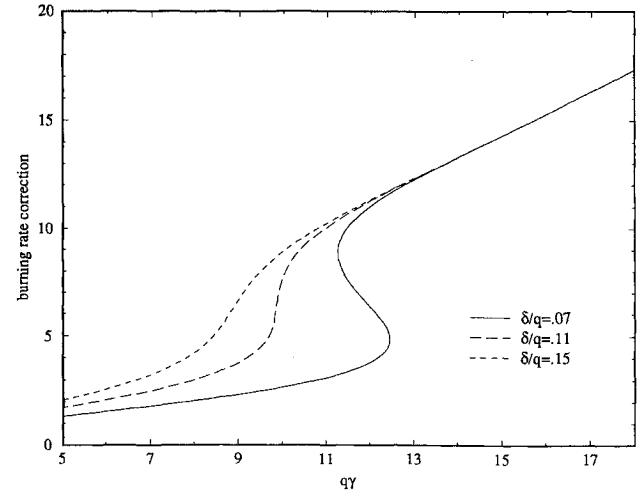

Fig. 3 Response curves: burning rate $M_1(1 - T_s + L)$ as a function of the scaled ambient oxidant concentration γ, for selected values of δ/q. Calculated for $M_0(1 - T_s + L) = 1, qM_0 = 4$, and $h = 0.05$.

smaller values of γ the response curve is monotonic. This change in shape of the response curve has significant implications regarding the dynamics of the flame. For example, the concept of abrupt extinction is associated with the S-shaped response curve. If the Damköhler number δ is slowly decreased, say in an experiment, the upper branch corresponding to an intense burning is followed down to the turning point. A further decrease in δ causes the response to jump to the lower branch, which corresponds to a weak burning, or a nearly extinguished state. The turning point is thus associated with extinction. In contrast, a monotonic response curve indicates that the transition from an intense to a weak burning state takes place in a gradual way. Indeed, behind this description is the assumption that the middle branch of the S curve is unstable and therefore cannot be realized in practice. The monotonic curve on the other hand is usually assumed to be stable for all δ. This last hypothesis is not necessarily true as shown next. One may also consider how the burning rate changes with the oxidant concentration, i.e., with γ. Response curves showing the dependence of the burning rate correction $(1-T_s+L)M_1$ on γq are shown in Fig. 3. For a fixed large value of δ the response is monotonic; the burning rate decreases gradually when the oxidant concentration in the ambient is continuously reduced. For smaller values of δ the response curve becomes S shaped, implying that abrupt extinction occurs as γ reaches a critical value γ_c. The preceding discussion regarding the distinction between the monotonic response and the S-shaped curve applies here as well.

V. Stability Analysis

To examine the stability of the steady states described earlier, we introduce temporal disturbances and write

$$\phi = \phi_s + \Phi(R)e^{\omega t}, \qquad y = y_s + \eta(R)e^{\omega t}, \qquad x = x_s + \chi(R)e^{\omega t}$$

with ω complex. In the following we restrict attention to equal and unity Lewis numbers, namely, $L_F = L_X = 1$. It is easily seen by subtracting Eqs. (14) and (15) that $\chi = \eta$. Equations (13) and (14) together with the boundary conditions (16) and (17) then yield the eigenvalue problem

$$\frac{1}{R^2}\frac{d}{dR}\left(R^2\frac{d\Phi}{dR}\right) + [q\delta x_s y_s e^{\phi_s} - (h+\omega)]\Phi = -q\delta e^{\phi_s}(x_s + y_s)\eta$$

$$\frac{1}{R^2}\frac{d}{dR}\left(R^2\frac{d\eta}{dR}\right) - [\delta(x_s + y_s)e^{\phi_s} + \omega)]\eta = \delta x_s y_s e^{\phi_s}\Phi \qquad (24)$$

$$R^2\frac{\partial\Phi}{\partial R} = R^2\frac{\partial\eta}{\partial R} = 0 \quad \text{as} \quad R \to 0$$

$$\Phi \to 0, \qquad \eta \to 0 \quad \text{as} \quad R \to \infty$$

for the determination of ω. A steady state $\{\phi_s, y_s, x_s\}$ is stable to infinitesimally small, spherically symmetric disturbances if $\Re(\omega) < 0$ for all of the eigenvalues. An instability develops when one of the eigenvalues, say ω, is such that $\Re(\omega) > 0$.

The system (24) was discretized using a central differences scheme, and the eigenvalues were found using the EISPACK routine. The interval length over which the equations were solved and the discretization size were chosen in an attempt to maximize the accuracy. A balance between the interval length and the discretization was chosen because of computational size limits; such a balance is obviously parameter dependent. This balance was chosen so that the qualitative nature of the results remains unchanged.

In the absence of radiation, $h = 0$, it can be shown (see Appendix) that all eigenvalues are real. Hence, if unstable modes exist, they will be nonoscillatory. Growing modes in this case are only observed along the middle branch of the S curves; the monotonic response curves are found to be always stable.

When the flame loses heat by radiation, or more specifically when h is above some critical value h_c, portions of the monotonic response curves may become unstable. For typical values of the parameters $M_0(1 - T_s + L)$ ranges between 0.5 and 2, and qM_0 ranges between 3 and 50. For representative values of these parameters it is shown in Fig. 4 that unstable states, corresponding to the dark segments of the response curves, exist for sufficiently large γ. Consider, for example, the response curve for $\gamma q = 12$ shown in Fig. 4a. For sufficiently large δ all of the eigenvalues have negative real parts implying stability: the Burke–Schumann flame sheet is unconditionally stable.

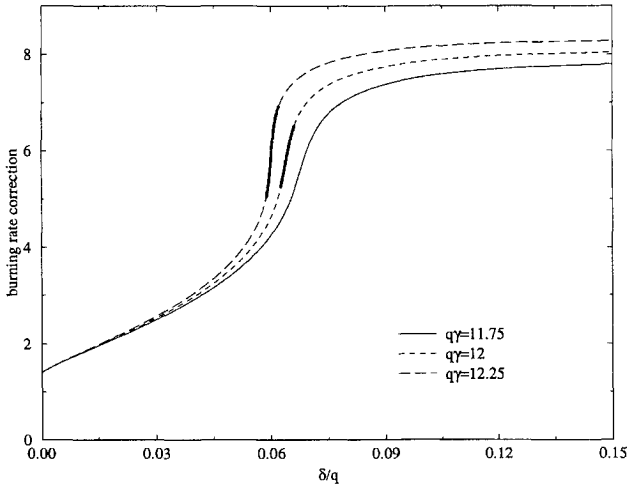

a) Calculated for $M_0(1 - T_s + L) = 2$, $qM_0 = 10$, and $h = 0.5$

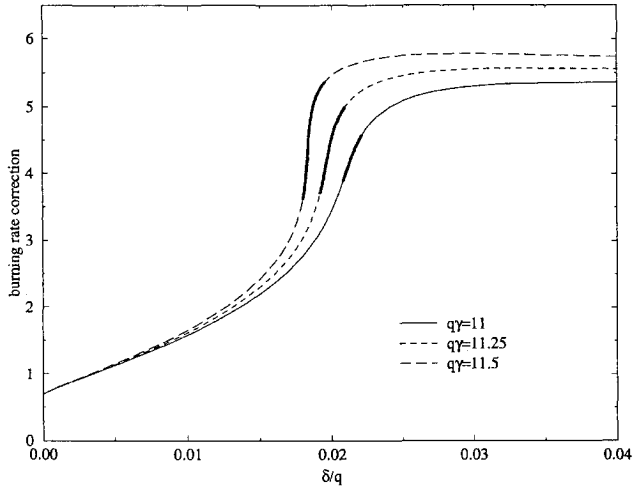

b) Calculated for $M_0(1 - T_s + L) = 1$, $qM_0 = 15$, and $h = 0.5$

Fig. 4 Unstable states along the response curves $M_1(1 - T_s + L)$ vs δ/q for selected values of $q\gamma$. The dark segments correspond to the unstable oscillatory states.

Table 1 Eigenvalues calculated for $M_0(1 - T_s + L) = 2$, $qM_0 = 10q\gamma = 12$, and $h = 0.5$[a]

δ/q	ω
0.0661	$0.0091 + 0.8878i$
0.0658	$0.0453 + 0.8314i$
0.0655	$0.0769 + 0.7736i$
0.0652	$0.1028 + 0.7161i$
0.0649	$0.1213 + 0.6618i$

[a]Neutral stability corresponds to $\delta/q \approx 0.06617$ and $\omega_c \approx 0.90082i$.

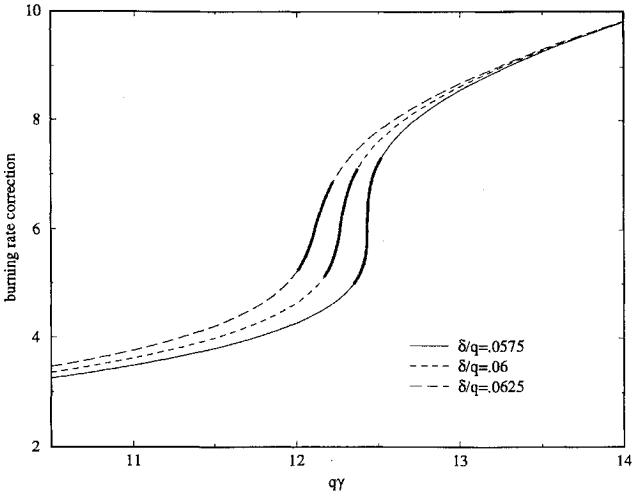

a) Calculated for $M_0(1 - T_s + L) = 2$, $qM_0 = 10$, and $h = 0.5$

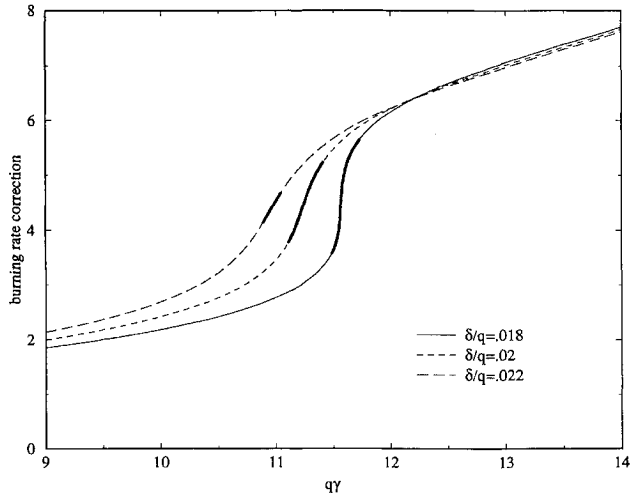

b) Calculated for $M_0(1 - T_s + L) = 1$, $qM_0 = 15$, and $h = 0.5$

Fig. 5 Unstable states along the response curves $M_1(1 - T_s + L)$ vs γq for selected values of δ/q. The dark segments correspond to the unstable oscillatory states.

By slowly decreasing δ a point, $\delta_c \simeq 0.06617\,q$ is reached where one of the eigenvalues $\omega = \omega_c \simeq 0.9008\,i$. Since $\Im(\omega_c) \neq 0$, the instability that develops upon reducing δ below δ_c is oscillatory in nature; $\Im(\omega_c)$ represents the frequency of oscillations. For $\delta < \delta_c$ one notes (see Tables 1 and 2) that the amplitude of oscillations grows more and more rapidly but only a small change in frequency results. Hence, by decreasing the Damköhler number below a critical value corresponding to δ_c, the burning becomes oscillatory with a frequency $\sim \Im(\omega_c)$. With a further decrease in the Damköhler number the growth rate increases until extinction occurs. Although the response curves in the figures appear to regain stability for sufficiently small δ, these states may never be observed in practice as they will most probably be superseded by extinction.

Unstable oscillatory modes are also found by gradually reducing the oxidant concentration in the ambient (Fig. 5). The response curves show the dependence of $(1 - T_s + L)M_1$ on γq for a fixed δ.

Table 2 Eigenvalues calculated for $M_0(1 - T_s + L) = 1, qM_0 = 15, q\gamma = 11.5$, and $h = 0.5$[a]

δ/q	ω
0.0195	$0.0019 + 0.7037i$
0.0193	$0.0575 + 0.6533i$
0.0191	$0.1153 + 0.5879i$
0.0189	$0.1746 + 0.5002i$
0.0187	$0.2328 + 0.3738i$

[a]Neutral stability corresponds to $\delta/q \approx 0.01951$ and $\omega_c \approx 0.70606i$.

Table 3 Eigenvalues calculated for $M_0(1 - T_s + L) = 2, qM_0 = 10, \delta/q = 0.06$, and $h = 0.5$[a]

$q\gamma$	ω
12.37	$0.0186 + 1.0175i$
12.35	$0.1074 + 0.8986i$
12.33	$0.1882 + 0.7597i$
12.31	$0.2565 + 0.5951i$
12.29	$0.3007 + 0.4013i$

[a]Neutral stability corresponds to $q\gamma \approx 12.3741$ and $\omega_c \approx 1.0410i$.

Table 4 Eigenvalues calculated for $M_0(1 - T_s + L) = 1, qM_0 = 15, \delta/q = 0.02$, and $h = 0.5$[a]

$q\gamma$	ω
11.41	$0.0139 + 0.6723i$
11.38	$0.0565 + 0.6217i$
11.35	$0.0947 + 0.5642i$
11.32	$0.1262 + 0.5015i$
11.29	$0.1476 + 0.4374i$

[a]Neutral stability corresponds to $q\gamma \approx 11.4196$ and $\omega_c \approx 0.6885i$.

The steady states are always stable when δ is large enough, as indicated earlier. Unstable states exist for $\delta < \delta_c$ as γq is lowered below a critical value. These states correspond to oscillatory burning consistent with the previous discussion (see also Tables 3 and 4).

VI. Results

The model discussed earlier describes the dynamics of a diffusion flame surrounding a liquid fuel droplet in a reduced oxidant environment ($X_\infty \ll 1$) and in the absence of gravity. What characterizes the system in this case is the absence of abrupt extinction conditions. Instead, a gradual decrease from intense to weak burning occurs, for a given oxidant concentration X_∞, as the Damköhler number is steadily reduced. A similar behavior occurs when the Damköhler number D is kept fixed but the oxidant concentration is reduced instead.

The transitional states, however, are not always stable. Here we have analyzed the effects of heat loss; effects as a result of differential diffusion will be discussed in a follow-up paper. The results indicate that in the presence of heat loss, or more specifically when $h > h_c$, unstable modes corresponding to oscillatory states develop when either the Damköhler number D or the ambient oxidant concentration X_∞ is reduced below some critical value. Consider, for example, a state corresponding to a given X_∞ and a sufficiently large D (see Fig. 4). The combustion field, manifested by a Burke–Schumann flame sheet, is absolutely stable. The chemical reaction is sufficiently fast so that, even if the flame is displaced slightly, complete combustion is quickly reestablished at a thin flame sheet located where fuel and oxidant meet at stoichiometric proportions. Heat loss has an insignificant effect in this case except for lowering the overall burning rate; see Eq. (23). By reducing D the flame broadens and moves outwards. The broader reaction zone is more sensitive to external disturbances because of the relatively smaller residence to chemical reaction time. If the reaction zone is displaced outwards, for example, its natural tendency is to reestablish itself near the unperturbed position. Because of heat loss, however, the flame temperature is reduced and consequently the chemical reaction time is increased. The effective Damköhler number is momentarily smaller so that the reaction zone moves outwards again. For small values of h these oscillations are damped, and the flame adjusts itself to its original position. When h exceeds h_c, however, the oscillations grow in magnitude. A new oscillatory state is established for $h \simeq h_c$. A similar behavior occurs when D is held fixed and X_∞ is gradually reduced (see Fig. 5).

The data in Tables 1–4 show that a relatively large increase in amplitude $\sim \exp[\Re(\omega)\, t]$ occurs as δ or γq is reduced below criticality. Consider a situation in which the oxidant concentration is continuously reduced. The flame, which at first is stable, develops instantaneous oscillations when X_∞ reaches a sufficiently low value. By further reducing the oxidant concentration, the amplitude of oscillations keeps on increasing, leading eventually to the extinguishment of the flame. This scenario is equivalent to what has been observed in the candle flame experiment, as reviewed in the Introduction.

The frequency of oscillations is given, in dimensional form, by

$$\Omega = \frac{\lambda}{\rho_\infty c_p a^2}\left(\frac{RT_\infty}{E}\right)^2 \Im(\omega)$$

For representative values of the physicochemical parameters, the critical value of the heat loss parameter, below which no oscillations develop, is found to be $h_c \sim 0.02 - 0.07$. Consider $h = 0.25$, for example, and an n-heptane droplet of diameter 1000μ burning in air. With $\mathcal{D}_{th} \simeq 2.71$ cm^2/s and $\epsilon \simeq 0.066$, and for $\gamma q = 12$–13, we find that the flame standoff distance is nearly 1.7–1.8 cm. Although this is somewhat larger than experimental flame-to-droplet radii, it is nevertheless within the range of typical theoretical predictions,[10] which are known to overestimate the flame standoff distance. For these conditions and for $\gamma q = 13$, we find that $\delta_c = 0.00700$ and consequently $\Im(\omega_c) = 0.3659$; for $\gamma q = 12.25$, we find $\delta_c = 0.00848$ and $\Im(\omega_c) = 0.2872$. Hence the predicted frequencies of oscillations $\Omega = 4.72\,\Im(\omega)$ are, respectively, 1.7 and 1.3 Hz.

Our numerical computations show that for a variety of conditions (see Tables 1–4) $\Im(\omega_c) \sim 0.5$–1.1. Hence, with a thermal diffusivity $\mathcal{D}_{th} \sim 2$–3 cm^2/s and a flame standoff distance ~0.5–2 cm, the predicted frequencies are in the range 0.7–1.5 Hz. In microgravity, candle flames have a standoff distance of nearly 5–8 mm (see Introduction). Hence, based on the present theory, one may expect that at the onset of instability the frequency of oscillations will be about 1 Hz, which is in clear agreement with the measured values.[2] We therefore conclude that near-limit oscillations, similar to the ones observed in the microgravity candle flame experiment, may result in the presence of heat loss.

Although oscillations have also been reported for candle flames in 1 g at relatively low pressures,[11] the observed frequencies in that case were much higher (6–9 Hz). It has been hypothesized that the oscillations in that case are related to the small convective buoyant flows that are always present on Earth, even at low Grashof numbers.

VII. Conclusions

We have examined the dynamics of a spherical diffusion flame in a reduced oxidant environment. In this case, the transition from intense burning, characterized by a Burke–Schumann flame sheet, to a weak-burning state is gradual. Whereas the Burke–Schumann flame sheet corresponding to a large Damköhler number is always stable, the transitional states for moderate Damköhler numbers may become unstable when heat losses are appreciable. The instability identified in this study is oscillatory in nature, with frequencies of the order of 1 Hz. The near-limit oscillations predicted here are qualitatively similar to the ones observed in the microgravity candle flame experiments as far as the conditions for their onset are concerned, and the frequencies of oscillations predicted are of the same order of magnitude. Unlike our predictions, however, the mode of oscillations observed in the experiments is not spherically symmetric.

Appendix: Proof that for $h = 0$ All Eigenvalues Are Real

When $h = 0$, the eigenvalue problem can be simplified by adding the equations for Φ and η, solving that equation, and then substituting in the equation for Φ to obtain

$$\frac{1}{R^2}\frac{\mathrm{d}}{\mathrm{d}R}\left(R^2\frac{\mathrm{d}\Phi}{\mathrm{d}R}\right) + \left[\delta e^{\phi_s}(q x_s y_s - x_s - y_s) - \omega\right]\Phi = 0$$

The boundary conditions remain as before. This eigenvalue problem is of a singular Sturm–Liouville type. Cross multiplying the equation with its complex conjugate counterpart, subtracting, and then integrating from zero to infinity yields

$$R^2\left\{\bar{\Phi}\frac{\mathrm{d}\Phi}{\mathrm{d}R}-\Phi\frac{\mathrm{d}\bar{\Phi}}{\mathrm{d}R}\right\}\Bigg|_{R=0}^{\infty}=(\omega-\bar{\omega})\int_0^{\infty}R^2|\Phi|^2\,\mathrm{d}R$$

where the bar denotes complex conjugate. The left-hand side of the equation vanishes at $R = 0$ in view of the boundary conditions. The behavior of Φ and $\bar{\Phi}$ for large R can be deduced in a similar way as done for the preceding ϕ_s, x_s, and y_s. One finds that Φ and $\bar{\Phi}$ decay exponentially fast to zero as $R \to \infty$. Since the left-hand side of this last equation vanishes, one concludes that $\Im(\omega) = 0$. Hence, if unstable growing modes corresponding to $\Re(\omega) > 0$ exist, they will necessarily be nonoscillatory.

Acknowledgments

This work was sponsored by the microgravity combustion program under NASA sponsorship and by the National Science Foundation. M. Matalon also acknowledges support from the United States–Israel Binational Science Foundation; Sally Cheatham acknowledges support from a National Science Foundation Graduate Research Fellowship. Thanks to H. Ross and D. Dietrich from NASA Lewis for their helpful comments and for the information they provided us regarding candle flames.

References

[1]Ross, H. D., Sotos, R. G., and Tien, J. S., "Observations of Candle Flames Under Various Atmospheres in Microgravity," *Combustion Science and Technology*, Vol. 75, Nos. 1–3, 1991, pp. 155–160.

[2]Dietrich, D., Ross, H. D., and Tien, J. S., "Candle Flames in Non-Buoyant and Weakly Buoyant Atmospheres," AIAA Paper 94-0429, Jan. 1994.

[3]Normandia, M. J., and Buckmaster, J. D., "Near-Asphyxiated Liquid Fuel Drop Burning," *Combustion and Flame*, Vol. 29, No. 3, 1977, pp. 277–282.

[4]Kirkby, L. L., and Schmitz, R. A., "An Analytical Study of the Stability of a Laminar Diffusion Flame," *Combustion and Flame*, Vol. 10, No. 3, 1966, p. 205.

[5]Buckmaster, J. D., "Edge Flames and their Stability," preprint, Dept. of Aeronautics and Astronautics, Univ. of Illinois–Urbana, IL, 1995.

[6]Penner, S. S., and Olfe, D. B., *Radiation and Reentry*, Academic, New York, 1968.

[7]Williams, F. A., *Combustion Theory*, Benjamin/Cummings, Menlo Park, CA, 1985.

[8]Matalon, M., and Law, C. K., "Gas Phase Transient Diffusion in Droplet Vaporization and Combustion," *Combustion and Flame*, Vol. 50, No. 2, 1983, pp. 219–229.

[9]Matalon, M., and Law, C. K., "Gas Phase Transient Diffusion in Droplet Vaporization and Combustion, Errata and Extension," *Combustion and Flame*, Vol. 59, No. 2, 1985, pp. 213–215.

[10]Law, C. K., "Recent Advances in Droplet Vaporization and Combustion," *Progress in Energy and Combustion Science*, Vol. 8, No. 3, 1982, pp. 169–199.

[11]Chan, W., and Tien, J., "An Experiment on Spontaneous Flame Oscillation Prior to Extinction," *Combustion Science and Technology*, Vol. 18, No. 3–4, 1978, pp. 139–143.